offset core (*17*) or a difference in crustal thickness between the near side and the far side (*15*).

W. L. SJOGREN
Jet Propulsion Laboratory, California Institute of Technology, Pasadena 91109
W. R. WOLLENHAUPT
NASA Manned Spacecraft Center, Houston, Texas 77058

References and Notes

1. R. Baldwin, *The Measure of the Moon* (Univ. of Chicago Press, Chicago, 1963).
2. Lunar Charts LAC 1 through LAC 144, Aeronautical Chart and Information Center, St. Louis, Mo.
3. W. L. Sjogren, in *Measure of the Moon*, Z. Kopal and C. L. Goudas, Eds. (Reidel, Dordrecht, Netherlands, 1967), pp. 341–343.
4. F. B. Winn, *Surveyor Project Final Report* (Technical Report 32-1265, Jet Propulsion Laboratory, Pasadena, Calif., 1968), part 2, pp. 407–438.
5. W. R. Wollenhaupt and G. A. Ransford, *Bull. Amer. Astron. Soc.* **3**, 272 (1971).
6. H. R. Compton and W. R. Wells, *Determination of Lunar Equatorial Radius Using Image-Motion Compensation Sensor Data from Lunar Orbiter I* (NASA TN D-5231, National Aeronautics and Space Administration, Washington, D.C., 1969).
7. A. Shapiro, E. A. Uliana, B. S. Yaplee, S. H. Knowles, in *Moon and Planets*, A. Dollfus, Ed. (North-Holland, Amsterdam, 1968), vol. 2, pp. 34–46.
8. W. R. Wollenhaupt, R. K. Osborn, G. A. Ransford, *Moon* **5** (Nos. 1/2), 149 (1972).
9. W. H. Michael, Jr., in *The Figure of the Moon* (NASA SP 201, National Aeronautics and Space Administration, Washington, D.C., 1969), pp. 63–64.
10. J. E. Faller *et al.*, in *Apollo 15 Preliminary Science Report* (NASA SP 289, National Aeronautics and Space Administration, Washington, D.C., 1971), pp. 14-1 to 14-6.
11. The L1 lunar gravity model is described by $GM\oplus = 4902.78$ km^3/sec^2 and the spherical harmonic coefficients $J_{20} = 2.07108 \times 10^{-4}$, $J_{30} = -0.21 \times 10^{-4}$, $C_{22} = 0.20716 \times 10^{-4}$, $C_{31} = 0.34 \times 10^{-4}$, and $C_{33} = 0.02583 \times 10^{-4}$.
12. The laser altimeter radius values agree very well with those obtained by Watts from limb outline measurements on photographic plates from the U.S. Naval Observatory (*1*).
13. B. N. Rodionov *et al.*, *Kosm. Issled.* **9**, 450 (1971).
14. W. R. Wollenhaupt and W. L. Sjogren, *Moon* **4** (Nos. 3/4), 337 (1972).
15. W. M. Kaula, G. Schubert, R. E. Lingenfelter, W. L. Sjogren, W. R. Wollenhaupt, in *Proceedings of the 3rd Lunar Science Conference* (M.I.T. Press, Cambridge, Mass., 1972), vol. 3, p. 2189.
16. S. K. Runcorn and M. H. Shrubsall, *Phys. Earth Planet. Interiors* **1**, 317 (1968).
17. G. A. Ransford and W. L. Sjogren, *Nature* **238**, 260 (1972).
18. Supported by NASA contract NAS 7-100.

6 October 1972

Source Parameters for Stick-Slip and for Earthquakes

Abstract. *Source parameters of stick-slip friction events measured in the laboratory show particle and rupture propagation velocities which are similar to those observed for earthquakes and inferred from seismic source theory. This dynamic similarity strongly supports the idea that stick-slip is the mechanism for shallow earthquakes.*

Brace and Byerlee (*1*) suggested stick-slip friction as a possible mechanism for shallow earthquakes because it produces jerky displacements and qualitatively explains, in terms of partial stress drops, the small stress release inferred for earthquakes compared with inherent rock strengths. We began a systematic laboratory study of the dynamic properties of stick-slip in order to understand more clearly the stick-slip mechanism and to suggest geophysical measurements that would indicate whether earthquake and stick-slip mechanisms are similar. Our results show that the dynamic behavior of stick-slip is nearly identical with that of earthquakes and provide a strong argument for the stick-slip model of shallow earthquakes.

These measurements were made with a new type of friction testing machine (*2*). The sample is a slab 10 by 18 by 3 cm, with a sliding surface formed by a ground cut made diagonally at 30° across its major face. The sample is placed in a biaxial load frame and loaded on two perpendicular edges with hydraulic rams, while the other edges are allowed to move freely on roller bearings in such a way as to allow unconstrained slip on the 30° "fault." Stresses are maintained uniform to within 10 percent along the entire fault and normal stresses up to about 1 kb are possible.

Particle velocity was measured directly across the fault by using either a differential capacitance displacement transducer or a linear variable resistor mounted directly on the specimen and across the central part of the fault. The velocities and general wave forms from the two different transducers agree well; thus, the transducer output faithfully reproduces the actual displacements. A typical curve of displacement as a function of time for a stick-slip event is shown in the lower right corner of Fig. 1. The displacement source time function is roughly a truncated ramp, with a gradual beginning and termination. The ramp systematically steepens with increasing stress drop (and hence total stress). The velocities were measured by fitting a straight line through the inclined section of the ramp by eye. The estimated errors in this procedure are about 10 percent.

Table 1. Rupture velocities, V_r, for stick-slip events at shear and normal stresses τ_1 and σ_1. The shear stress drop is $\Delta\tau$.

V_r (km/sec)	σ_1 (bars)	τ_1 (bars)	$\Delta\tau$ (bars)
2.3	27	16	5
2.4	26	15	6
3.0	35	24	8
3.3	237	90	19
3.5	252	94	23
4.1	257	102	32
4.0	280	94	20
4.7	291	114	50
4.7	320	101	30
4.7	351	125	22
4.7	363	115	40
3.5	361	122	39
4.6	383	127	47
4.8	395	143	52
4.7	420	147	49

The rupture velocity was measured by photographing the output of four axial piezoelectric transducers (accelerometers) displayed on an oscilloscope. The transducers were spaced evenly at 3-cm intervals along one side of the fault and at 5 mm from the fault edge. The passage of the rupture front was visible as a large pulse with a relatively long period followed by a higher frequency coda. The propagation time between different transducers was measured by using the first sharp break in the signal and the velocities computed. The velocities obtained between different transducers agreed within the assigned experimental error of about ± 15 percent, which was largely based on difficulties in choosing the first break. Richards (*3*) suggests that a large acceleration may occur before the passage of the rupture front, thus making its identification difficult, but as long as the recorded acceleration pulse shapes are uniform along the fault the rupture velocity will be correctly measured. Changes in the acceleration pulse shape along the fault were occasionally observed, but rupture velocities were only measured from uniform signals. Our observations are that the rupture accelerates to its terminal velocity very rapidly, that is, within about 3 cm. This contrasts with a fracture in virgin rock, which takes 20 to 30 cm to reach its terminal velocity (*4*).

Figure 1 and Table 1 present laboratory measurements of particle velocity and rupture velocity as a function of stress and stress drop for stick-slip between ground (80-grit wheel) surfaces of Westerly granite. The particle velocities (one half the velocity of one side of the fault with respect to the other)

vary from about 2 to 50 cm/sec and increase systematically with shear stress drops of about 1 to 40 bars. The shear stress drop is always about 10 percent of the total shear stress. The rupture velocities vary from about 2.3 to 4.8 km/sec. Although the data are limited there is a suggestion of increased rupture velocity with increased stress drop.

Particle velocities obtained from strong-motion instruments located near earthquake epicenters range from 10 to just over 100 cm/sec (*5, 6*), in excellent agreement with our experimental results. No direct measurements of stress drops resulting from earthquakes exist, but theoretical relations (*6–8*) suggest stress drops in the range of a few bars to hundreds of bars, again in good agreement with the experimental data.

The straight line in Fig. 1 is the relation between particle velocity and stress drop predicted by Brune (*7*) and calculated by using the elastic constants for Westerly granite (*9*). For comparison, we assume here that the effective stress (the difference between the static shear stress just before stick-slip and the stress resisting movement during slip) as referred to in the theory is equal to the stress drop. The general agreement in Fig. 1 is quite good; however, preliminary experiments in which we used different thicknesses of gouge on the fault surface indicate that the slope of the curve for particle velocity plotted against stress drop is a function of the conditions on the surface of the fault. This presents a further complication not considered in Brune's model. Although our experimental results support Brune's model, the agreement may be fortuitous since the effective stress is equal to the stress drop only in special circumstances, that is, for a particular value of the seismic radiation efficiency [about 5 percent (*2*)]. The effective stress cannot presently be measured, hence a direct test of the theory cannot be made. Still, the general agreement shown in Fig. 1 is encouraging in that it suggests that Brune's seismic source theory is probably at least not far wrong (although he does not consider the more complicated case of a propagating source).

At 250 bars confirming pressure, the shear velocity, V_s, is about 3 km/sec and the particle velocity, V_p, is about 5.1 km/sec in Westerly granite (*9*); thus, the rupture velocities, V_r (Table 1), are subshear to transonic ($V_s < V_r < V_p$). Wu *et al.* (*10*), using an entirely different experimental arrangement,

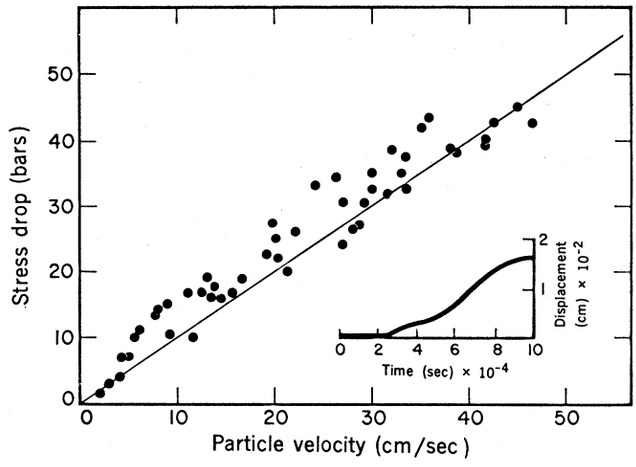

Fig. 1. Particle velocity as a function of stress drop for stick-slip events with Westerly granite. The straight line is predicted by Brune's theory (*7*). Inset shows a typical displacement-time function for an event.

also report subshear to transonic rupture velocities for stick-slip in Plexiglas. On the basis of model experiments for materials in tension and theoretical studies of crack propagation (*11*), most seismologists have assumed that earthquakes propagate at about the shear wave velocity or less, although Weertman (*12*) has proposed models in which transonic or supersonic rupture velocities are allowed. There is no strong seismic evidence for a shear wave velocity limit to rupture propagation. Kanamori (*13*) presented data from an earthquake in the Kurile Islands in 1963 which were best fit by a transonic rupture velocity (4.5 km/sec); in other studies [for example, (*5, 6, 14*)] velocities of about 2.5 to 3.5 km/sec have been suggested. The *S* wave velocity in the upper crust ranges from about 3.4 to 3.7 km/sec; thus, the observed rupture velocities are subshear to transonic. However, these velocities are somewhat arbitrary since V_r is inseparable from the effect of fault length. Also, these rupture velocities are averages for earthquakes with complex wave forms, which suggest that the rupture front slowed and accelerated. If this occurs, the average velocity observed is less than the maximum rupture velocity. We believe that our experimental data are in good agreement with the seismic data on rupture velocity.

It is interesting that Weertman's (*12*) transonic propagation model requires that the fault be creeping (that is, stably sliding) prior to stick-slip. Our measurements (*2*) show, in fact, that the entire fault is creeping prior to stick-slip in these experiments, and at a rapidly accelerating rate. This implies that the entire fault is under stress high enough to produce slip. One possible way of producing transonic rupture velocities might be the following: After failure of some section of the fault by crack growth at about V_s, the radiated *P* waves trigger rupture on isolated areas ahead of the rupture front, but not everywhere, due to small-scale inhomogeneities in the stress and strength distribution on the fault. Thus, the average velocity of the rupture front could lie between the *S* and *P* wave velocities.

Although the dynamic properties of stick-slip propagation in different rock types have yet to be measured, the initial results for Westerly granite are so encouraging that we think stick-slip must be considered seriously as the mechanism of shallow earthquakes. Since stick-slip is readily observable in the laboratory, a rapid advance in understanding the basis of the earthquake mechanism is possible in the near future.

TRACY JOHNSON
Lamont-Doherty Geological Observatory of Columbia University, Palisades, New York 10964
FRANCIS T. WU
Department of Geology, State University of New York, Binghamton
CHRISTOPHER H. SCHOLZ
Lamont-Doherty Geological Observatory

References and Notes

1. W. F. Brace and J. D. Byerlee, *Science* **153**, 990 (1966).
2. C. Scholz, P. Molnar, T. Johnson, *J. Geophys. Res.*, in press.
3. P. G. Richards, *Abstracts with Program* (Seismological Society of America Meeting, Honolulu, 1972), vol. 4, p. 224.
4. Z. Bieniawski, *Felsmechanik Ingenieurgeol.* **6**, 113 (1968).
5. M. Wyss and T. Hanks, *Bull. Seismol. Soc. Amer.* **62**, 591 (1972).
6. M. D. Trifunac, *ibid.*, p. 721.
7. J. N. Brune, *J. Geophys Res.* **75**, 4997 (1970).
8. C. B. Archambeau, *Rev. Geophys.* **6**, 241 (196→ R. Burridge, *Phil. Trans. Roy. Soc. London Ser. A* **265**, 353 (1969); K. Aki, *Bull. Earthquake Res. Inst. Univ. Tokyo* **44**, 73 (1966).

9. F. Birch, in *Handbook of Physical Constants* (Memoir 97, Geological Society of America, Boulder, Colo., 1966), p. 97.
10. F. Wu, K. C. Thomson, H. Kuenzler, *Bull. Seismol. Soc. Amer.*, in press.
11 F. Erdogan, in *Fracture*, H. Liebowitz, Ed. (Academic Press, New York, 1968), vol. 2, p. 498.
12. J. Weertman, *J. Geophys. Res.* **74**, 6617 (1969).
13. H. Kanamori, *ibid.* **75**, 5011 (1970).
14. A. Ben-Menahem and N. Toksöz, *Bull. Seismol. Soc. Amer.* **53**, 905 (1963).
15. Supported by grant GA 21472 from the National Science Foundation and grant N22-201-72G from the National Oceanic and Atmospheric Administration. Lamont-Doherty Geological Observatory Contribution No. 1821.

6 October 1972; revised 15 November 1972

The Hydroperoxyl Radical in Atmospheric Chemical Dynamics: Reaction with Carbon Monoxide

Abstract. *From measurements of the photochemical rate of production of $CO_2^{16,18}$ and $CO_2^{16,16}$, produced from the low intensity photolysis of mixtures of CO, H_2O, Ar, and $O_2^{18,18}$, the rate constant for the reaction $HO_2 + CO \rightarrow CO_2 + OH$ has been determined at 300°K to be less than or equal to 10^{-20} cubic centimeter per molecule per second. These measurements indicate that the reaction of thermalized HO_2 is of negligible importance as a sink mechanism for converting CO to CO_2 in either the troposphere or the stratosphere.*

The transient species HO_2 has long been postulated to play an important role in atmospheric chemistry (*1*). Of considerable interest has been the reaction sequence 1, 2, and 3

$$HO_2 + CO \rightarrow CO_2 + OH \quad (1)$$
$$OH + CO \rightarrow CO_2 + H \quad (2)$$
$$H + O_2 + M \rightarrow HO_2 + M \quad (3)$$

where M is a third body. This chain sequence would represent a very efficient mechanism for conversion of CO to CO_2 in the atmosphere. The possible importance of this coupled set of reactions, however, depends on whether or not the rates of the above processes are greater than those for possible competing reactions involving the transient species H, OH, and HO_2. Essential to this evaluation, therefore, are the rate constants for reactions 1, 2, and 3, as well as for possible competing reactions. With regard to reactions 2 and 3 and several other atmospheric reactions of H and OH, the rate constants are reasonably well known for purposes of this evaluation (*2*). In the case of reaction 1 and other competing reactions involving the HO_2 species, the situation is much less satisfactory. In fact, until quite recently, the only available rate constant for reaction 1 was that provided by Baldwin *et al.* (*3*), who calculated the value of k_1 at temperatures in the vicinity of 770°K from measurements of the rate constant ratio k_1/k_4. Reaction 4 in this system was the disproportionation reaction

$$HO_2 + HO_2 \rightarrow H_2O_2 + O_2 \quad (4)$$

An extrapolation of these rate data (*4*) to 300°K yields a value of approximately 10^{-24} cm^3 molec^{-1} sec^{-1} for k_1.

More recently Westenberg and de Haas (*5*) have estimated a rate constant for reaction 1 at 300°K of approximately 1×10^{-12} cm^3 molec^{-1} sec^{-1}, 12 orders of magnitude greater than Baldwin's estimate. Westenberg (*6*) has suggested, therefore, that the coupled set of reactions 1, 2, and 3 do, in fact, represent an efficient sink for the conversion of CO to CO_2. Westenberg's measurements further imply that the efficient conversion of CO to CO_2 could take place even in the absence of nitric oxide. Our purpose here is to report on recent measurements in our laboratory which indicate that reaction 1 cannot be of significance in defining the chemical dynamics of either the troposphere or the stratosphere.

In most of the experiments in this study, the production of HO_2 was via the third order reaction 3. Recent measurements in our laboratory by the flash photolysis–resonance fluorescence technique have given the absolute rate constant for this reaction at 300°K as 1.95×10^{-32} cm^6 molec^{-2} sec^{-1} for M = Ar and 5.26×10^{-32} cm^6 molec^{-2} sec^{-1} for M = N_2 (*7*). Foner and Hudson (*8*) have also detected the HO_2 radical mass spectrometrically when produced from reaction 3, thus demonstrating the production of this species in the H-O_2-M system. In a limited number of experiments, we generated HO_2 via the photolysis of H_2O_2. In this system, an excess of H_2O_2 over CO ensured that most of the initially formed OH reacted with H_2O_2 to produce HO_2; for example

$$H_2O_2 + h\nu \rightarrow 2OH \quad (5)$$
$$OH + H_2O_2 \rightarrow HO_2 + H_2O \quad (6)$$

Foner and Hudson (*8*) also obtained direct mass spectrometric evidence indicating the formation of HO_2 from the photolysis of H_2O_2. The mechanism of formation was believed to be that of reactions 5 and 6.

The experimental apparatus used in this study consisted of a 300-cm^3 Pyrex photolysis cell equipped with a 1-inch Suprasil window (transmitting wavelengths above 1650 Å), a Hg resonance lamp, and a high-vacuum (10^{-6} mm) submanifold system through which the gases H_2O, CO, $O_2^{18,18}$, and Ar could be metered into the photolysis cell. The output of the Hg resonance lamp was examined on a vacuum ultraviolet monochromator and was found to consist of nearly equal amounts of the two lines, 1849 and 2537 Å. In these experiments, no attempt was made to block the 2537-Å line since neither the reactants (H_2O, CO, O_2, Ar) nor the product (CO_2) absorbed significantly at this wavelength. Blank experiments with H_2O absent from the photolysis mixture indicated that production of CO_2 from mechanisms involving reactive species other than OH and HO_2 (*9*) was always less than 2 percent of the total product CO_2 observed. Analysis of the products, $CO_2^{16,18}$ and $CO_2^{16,16}$, was carried out by using a mass spectrometer (Consolidated Electrodynamics Corporation model 21-620). All reactants used in these experiments were research grade and had stated purities of 99+ percent. Both the CO and the $O_2^{18,18}$ were passed slowly through a liquid N_2 cold trap filled with glass beads before being used in photolysis experiments. In the case of CO, traces of iron carbonyl and CO_2 were removed. For $O_2^{18,18}$ small amounts of $CO_2^{18,18}$ had to be separated from the oxygen. Blank experiments carried out at the highest pressures of CO and Ar used in the reported experiments showed the residual CO_2 pressure al-

Table 1. Data for the reaction of HO_2 with CO. The concentrations of the reactants were 20 torr H_2O and 1 torr $O_2^{18,18}$. The total pressure was 200 torr (Ar + CO) and the photolysis time approximately 14 minutes at an intensity of 3×10^{14} photons cm^{-2} sec^{-1}. The total yield of CO_2 was 8 to 14 mtorr. In blank experiments the yield of CO_2 was about 0.4 mtorr. The reproducibility of the results was ± 15 percent; the results presented here are the averages from 25 experiments.

CO (torr)	Relative yield	
	$CO_2^{16,16}$	$CO_2^{18,18}$
1	100	6.3
10	100	6.8
40	100	6.2
150	100	6.4